Adv. Studies Theor. Phys., Vol. 6, 2012, no. 15, 743 - 753

Fluid Flow and Heat Transfer in Square Cavities with Discrete Two Source-Sink Pairs

Achariya Namprai

Department of Mathematics, Faculty of Science,
Khon Kaen University, Khon Kaen 40002, Thailand
jam_acha@hotmail.com

Supot Witayangkurn*

Department of Mathematics, Faculty of Science,
Khon Kaen University, Khon Kaen 40002, Thailand
supot_wa@kku.ac.th

Abstract

This research presents the fluid flow and heat transfer characteristics of natural convection in a two-dimensional square cavity with discrete two source–sink pairs on the vertical sidewalls obtained from investigating isotherms, streamlines, and heatlines. The arrangement of the sources and sinks are changed from the separated to staggered modes. A finite element method is used for solving the governing equations. The interested parametric are Darcy number in the range of 10^{-6} to 10^{-1}, Rayleigh number constant at 10^{6}, and Prandtl number constant at 0.71. The numerical solutions are calculated by using FlexPDE 6.14 Student Version and displayed in terms of isotherms, streamlines, and heatlines. It is found that the heat transfer is related with the number of eddies in the enclosure. When the sources and sinks were split into smaller segments and arranged in a staggered mode, the number of eddies in the enclosure increase.

Mathematics Subject Classification: 65N30, 35Q30

Keywords: Discrete two source–sink pairs, Finite element method, Governing equations, Natural convection

*Corresponding Author

1 Introduction

The study of natural convection heat flows in an enclosure with discrete heat sources has been widely attended. This phenomenon has been applying to many scientific and engineering applications such as electronics cooling, food storage, and passive cooling of buildings. By using this approach, the hot-spot temperature in the enclosure will be decreased.

This work is related to natural convection in square cavity. Earlier studies concentrate on this topic with one source and one sink [1]. It was found that both the size and location of the discrete heat source significantly influence the behavior of heat transfer. Recently, researches in this type of problem have been extended to investigate the behavior of natural convection due to multiple discrete source-sink pairs; for example, see [2,3].

For the natural convection flows in a square cavity filled with a porous matrix, Basak et al. [2], studied numerically using penalty finite element method for uniformly and non-uniformly heated bottom wall, and adiabatic top wall maintaining constant temperature of cold vertical walls. Darcy–Forchheimer model is used to simulate the momentum transfer in the porous medium. This study yields consistent performance over a wide range of parameters, Rayleigh numbers $(Ra = 10^3 - 10^6)$, Darcy numbers $(Da = 10^{-5} - 10^{-3})$ and Prandtl numbers $(Pr = 0.71 - 10)$ with respect to continuous and discontinuous thermal boundary conditions. Consequently, the complicated heat transfers in enclosures with multiple sources and sinks are also studied. Deng [3] introduced the concept of heat function and its contour lines, heatlines, are currently adopted to visualize the heat transport process induced by convection. From above, we found that many researchers study about the effects of some parameters with different thermal boundary conditions and different shape. They attempt to analyze fluid flow and heat transfer by investigate isotherms, streamlines, and heatlines. Furthermore, the study of heatline approach, Kaluri et al. [4], is implemented to visualize heat transfer and to study efficient thermal mixing of laminar natural convective flow in a square cavity with distributed heat sources. Four different cases depending upon the location of the heat sources on the walls of the cavity are studied. Wide range of Prandtl number $(Pr = 0.015 - 1000)$ is studied over a range of Rayleigh number $(Ra = 10^3 - 10^5)$.

This research has studied the characteristic of the fundamental fluid flow and heat transfer for natural convection in a two-dimensional square cavity with discrete two source–sink pairs on the vertical sidewalls. The arrangement of the sources and sinks changes from the separated mode to staggered modes, i.e., first sources and sinks are separately located on two sidewalls, then they are alternately located on two sidewalls, and finally they are alternately located on one sidewall. Main attentions are focused on the significant effects of parameters, Darcy number $(Da = 10^{-6} - 10^{-1})$, Rayleigh number $(Ra = 10^6)$, and Prandtl number $(Pr = 0.71)$ and location of discrete source–sink pairs on the flow structure in the enclosures and hence overall heat transfer.

2 Mathematical Formulation

2.1 Velocity and temperature distributions

The physical model under investigation in Figure 1, is a square cavity of height L with discrete two source–sink pairs on the vertical sidewalls. The heat sources are maintained at a constant temperature T_h, higher than that of the sinks T_c $(T_c < T_h)$. Other parts of the enclosures are all thermally insulated. The arrangement of the sources and sinks has great impact on the fluid flow structures in the enclosure as follows:

Case 1. Only one eddy will be formed in the enclosure.
Case 2. There will be two eddies in the enclosure.
Case 3. Four eddies will be formed in the enclosure.

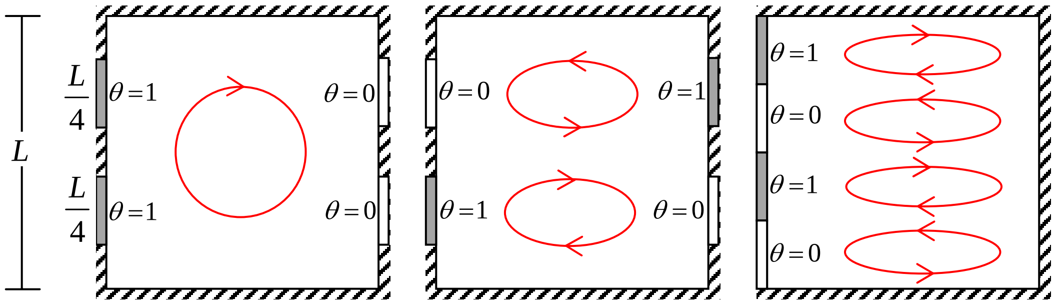

Case 1 Case 2 Case 3

Figure 1. Schematic diagram of the physical system

The fluid is considered as incompressible, newtonian and the flow is assumed to be laminar. The governing equations for steady two-dimensional natural convection flow in the porous cavity using conservation of mass, momentum and energy can be written as:

$$\frac{\partial u}{\partial x}+\frac{\partial v}{\partial y}=0, \tag{1}$$

$$u\frac{\partial u}{\partial x}+v\frac{\partial u}{\partial y}=-\frac{1}{\rho}\frac{\partial p}{\partial x}+\nu\left(\frac{\partial^2 u}{\partial x^2}+\frac{\partial^2 u}{\partial y^2}\right)-\frac{\nu}{K}u, \tag{2}$$

$$u\frac{\partial v}{\partial x}+v\frac{\partial v}{\partial y}=-\frac{1}{\rho}\frac{\partial p}{\partial y}+\nu\left(\frac{\partial^2 v}{\partial x^2}+\frac{\partial^2 v}{\partial y^2}\right)-\frac{\nu}{K}v+g\beta\left(T-T_c\right), \tag{3}$$

$$u\frac{\partial T}{\partial x}+v\frac{\partial T}{\partial y}=\alpha\left(\frac{\partial^2 T}{\partial x^2}+\frac{\partial^2 T}{\partial y^2}\right), \tag{4}$$

where

x, y	the distances measured along the horizontal and vertical directions,
u, v	the velocity components in the x and y directions,
ρ	density $(kg \cdot m^{-3})$,
p	pressure (Pa),
ν	kinematic viscosity $(m^2 \cdot s^{-1})$,
K	permeability of the porous medium,
g	acceleration due to gravity $(m^2 \cdot s^{-1})$,
α	thermal diffusivity $(m^2 \cdot s^{-1})$,
β	volume expansion coefficient (K^{-1}),
T	temperature (K).

We set the following change of variables:

$$X = \frac{x}{L}, \qquad Y = \frac{y}{L}, \qquad U = \frac{uL}{\alpha}, \qquad V = \frac{vL}{\alpha}, \qquad \theta = \frac{T - T_c}{T_h - T_c},$$

$$P = \frac{pL^2}{\rho\alpha^2}, \qquad Pr = \frac{\nu}{\alpha}, \qquad Da = \frac{K}{L^2}, \qquad Ra = \frac{g\beta\left(T_h - T_c\right)L^3 Pr}{\nu^2}, \tag{5}$$

where

X, Y	dimensionless distance along coordinate x and y,
U, V	dimensionless velocity components in the X and Y directions,
θ	dimensionless temperature,
P	dimensionless pressure,
Pr	Prandtl number,
Da	Darcy number,
Ra	Rayleigh number.

Then the governing equations (1)–(4) reduce to non-dimensional form:

$$\frac{\partial U}{\partial X} + \frac{\partial V}{\partial Y} = 0, \tag{6}$$

$$U\frac{\partial U}{\partial X} + V\frac{\partial U}{\partial Y} = -\frac{\partial P}{\partial X} + Pr\left(\frac{\partial^2 U}{\partial X^2} + \frac{\partial^2 U}{\partial Y^2}\right) - \frac{Pr}{Da}U, \tag{7}$$

$$U\frac{\partial V}{\partial X} + V\frac{\partial V}{\partial Y} = -\frac{\partial P}{\partial Y} + Pr\left(\frac{\partial^2 V}{\partial X^2} + \frac{\partial^2 V}{\partial Y^2}\right) - \frac{Pr}{Da}V + RaPr\theta, \tag{8}$$

$$U\frac{\partial \theta}{\partial X} + V\frac{\partial \theta}{\partial Y} = \left(\frac{\partial^2 \theta}{\partial X^2} + \frac{\partial^2 \theta}{\partial Y^2}\right). \tag{9}$$

The boundary conditions for velocities are:

$$U\left(X,0\right) = U\left(X,1\right) = U\left(0,Y\right) = U\left(1,Y\right) = 0,$$

$$V\left(X,0\right) = V\left(X,1\right) = V\left(0,Y\right) = V\left(1,Y\right) = 0, \tag{10}$$

and the boundary conditions for temperature are:

$$\theta = 1 \qquad \text{(for sources)},$$
$$\theta = 0 \qquad \text{(for sinks)},$$
$$\frac{\partial \theta}{\partial Y} = 0 \qquad \text{(for adiabatic walls)}. \tag{11}$$

The continuity equation (Eq. (6)) has been used as a constraint due to mass conservation and this constraint may be used to obtain the pressure distribution. In order to solve Eqs. (7) and (8), we use the penalty finite element method where the pressure P is eliminated by a penalty parameter γ and the incompressibility criteria given by Eq. (6) (see [5]) which results in

$$P = -\gamma \left(\frac{\partial U}{\partial X} + \frac{\partial V}{\partial Y} \right). \tag{12}$$

The continuity equation (Eq. (6)) is automatically satisfied for large values of γ. Typical value of γ that yields consistent solutions is 10^7; see [4]. Using Eq. (12), the momentum balance equations (Eqs. (7) and (8)) reduce to

$$U \frac{\partial U}{\partial X} + V \frac{\partial U}{\partial Y} = \gamma \frac{\partial}{\partial X} \left(\frac{\partial U}{\partial X} + \frac{\partial V}{\partial Y} \right) + Pr \left(\frac{\partial^2 U}{\partial X^2} + \frac{\partial^2 U}{\partial Y^2} \right) - \frac{Pr}{Da} U \tag{13}$$

and

$$U \frac{\partial V}{\partial X} + V \frac{\partial V}{\partial Y} = \gamma \frac{\partial}{\partial Y} \left(\frac{\partial U}{\partial X} + \frac{\partial V}{\partial Y} \right) + Pr \left(\frac{\partial^2 V}{\partial X^2} + \frac{\partial^2 V}{\partial Y^2} \right) - \frac{Pr}{Da} V + RaPr\theta. \tag{14}$$

2.2 Stream function

The fluid motion is displayed by using the stream function ψ obtained from velocity components U and V. The relationships between stream function and velocity components for two dimensional flows [4] are

$$U = \frac{\partial \psi}{\partial Y} \qquad \text{and} \qquad V = -\frac{\partial \psi}{\partial X}, \tag{15}$$

which yield a single equation

$$\frac{\partial^2 \psi}{\partial X^2} + \frac{\partial^2 \psi}{\partial Y^2} = \frac{\partial U}{\partial Y} - \frac{\partial V}{\partial X}. \tag{16}$$

The sign convention is as follows: positive sign of ψ denotes anticlockwise circulation and clockwise circulation is represented by the negative sign of ψ. The no-slip condition is valid at all boundaries as there is no cross flow, hence the boundary condition for stream function is

$$\psi = 0. \tag{17}$$

2.3 Heat function

The heat flow within the enclosure is displayed by using the heat function Π obtained from conductive heat fluxes $\left(-\frac{\partial\theta}{\partial X},-\frac{\partial\theta}{\partial Y}\right)$ as well as convective heat fluxes $(U\theta,V\theta)$. The heat function satisfies the steady energy balance equation (Eq. (9)) [7] such that

$$\frac{\partial\Pi}{\partial Y}=U\theta-\frac{\partial\theta}{\partial X} \quad \text{and} \quad -\frac{\partial\Pi}{\partial X}=V\theta-\frac{\partial\theta}{\partial Y}, \tag{18}$$

which yield a single equation

$$\frac{\partial^2\Pi}{\partial X^2}+\frac{\partial^2\Pi}{\partial Y^2}=\frac{\partial}{\partial Y}(U\theta)-\frac{\partial}{\partial X}(V\theta). \tag{19}$$

The basis of sign convention for heat function is based on the concept that heat flows from hot to cold surface and positive heat function corresponds to anti-clockwise heat flow. The boundary conditions for heat function are:

$$\begin{aligned}
&\frac{\partial\Pi}{\partial Y}=\pi cos(\pi Y) && \text{(for sources)},\\
&\frac{\partial\Pi}{\partial X}=0 && \text{(for sinks)},\\
&\Pi=0 && \text{(for adiabatic walls)}.
\end{aligned} \tag{20}$$

Using the above definition of the heat function, the positive sign of Π denotes anti-clockwise heat flow and the clockwise heat flow is represented by the negative sign of Π.

3 Results and Discussion

In this results, the fluid flow, heat transfer and the procedure discussed previously are taken from FlexPDE 6.14 Student Version. Original graphic output are modified from FlexPDE 6.14 Student Version to illustrate isotherms, streamlines, and heatlines. During the computations, the Prandtl number and the Rayleigh number are kept constant as $Pr=0.71$ and $Ra=10^6$ respectively, but the Darcy number is varied within the range $Da=10^{-6}-10^{-1}$. Different

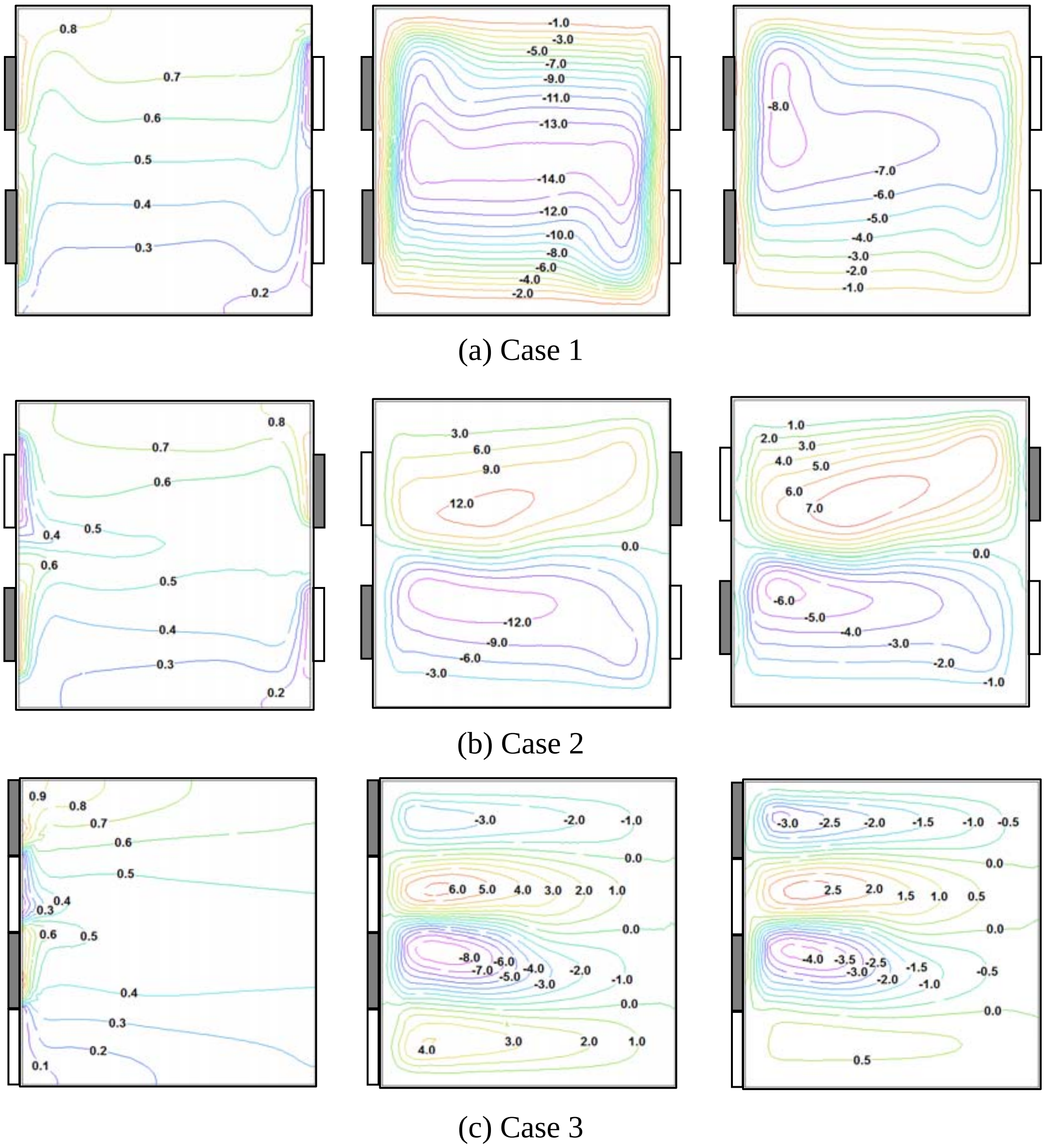

Figure 2. Isotherms (left), streamlines (center), and heatlines (right) for different arrangement of two source–sink pairs with $Ra = 10^6$, $Pr = 0.71$ and $Da = 10^{-1}$

arrangements of the sources and sinks and their effects are investigated.

Figure 2 shows the fluid flow and heat transfer characteristics and also heat transport with $Ra = 10^6$, $Pr = 0.71$ and $Da = 10^{-1}$. For Case 1, the sources and sinks are separately located on two sidewalls, and their buoyancies are thus composed together, which creates only one eddy in the enclosure, i.e., the fluid is driven upward by the sources on the left sidewall and then downward by the sinks on the right sidewall. Heatlines illustrate a different heat transport process and on

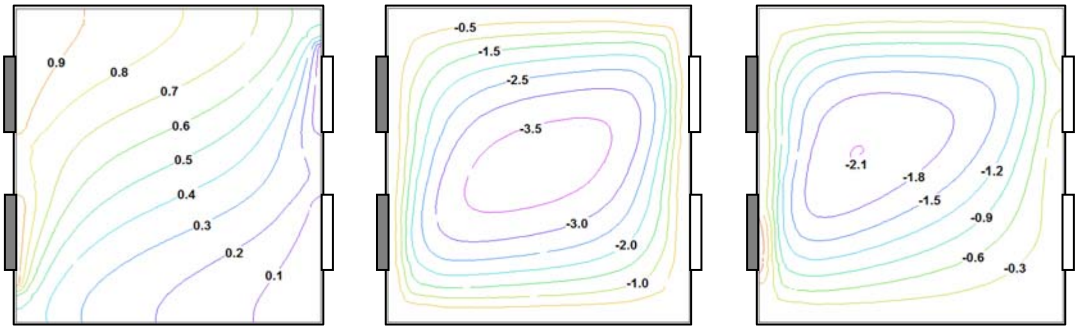

(a) Case 1

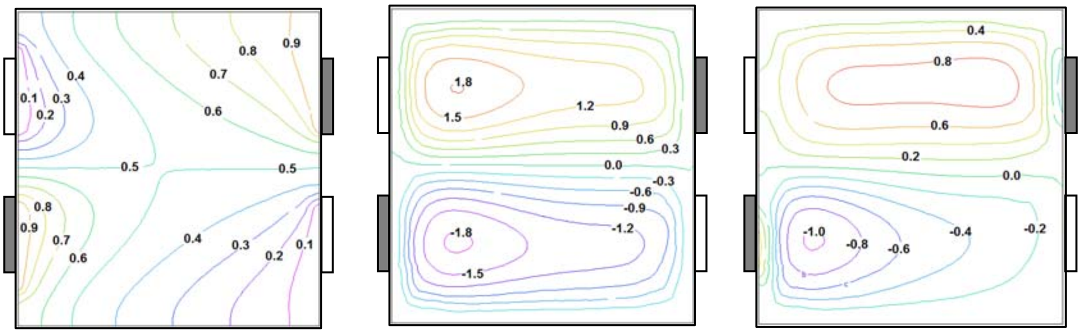

(b) Case 2

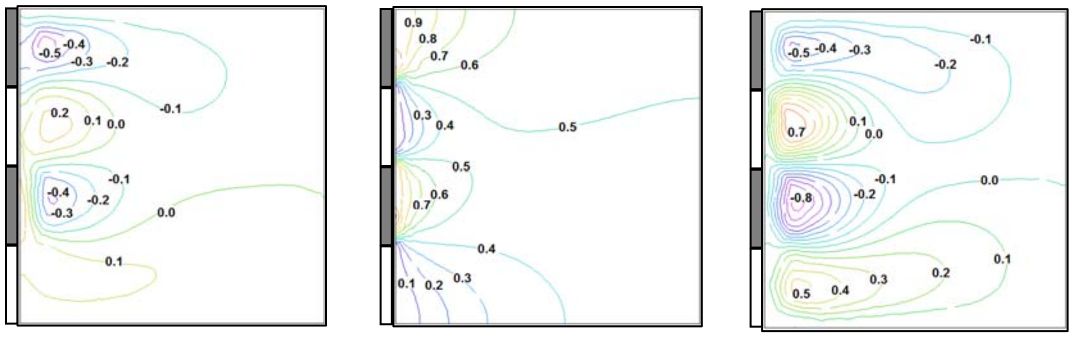

(c) Case 3

Figure 3. Isotherms (left), streamlines (center), and heatlines (right) for different arrangement of two source–sink pairs with $Ra = 10^6$, $Pr = 0.71$ and $Da = 10^{-4}$

the right sidewall. Heatlines illustrate a different heat transport process and demonstrate that more heat is transferred from the bottom source than the top source. For Case 2, because the sources and sinks are alternately located on two sidewalls, their buoyancies are decomposed into two groups, which generate two eddies, one anti-clockwise eddy set up by the source–sink pair in the upper region and another clockwise eddy in the lower region, as shown by streamlines. Heatlines show that the heat from the top source is channeled by the upper anti-clockwise flow to the top sink on the opposite side. The heat from the bottom

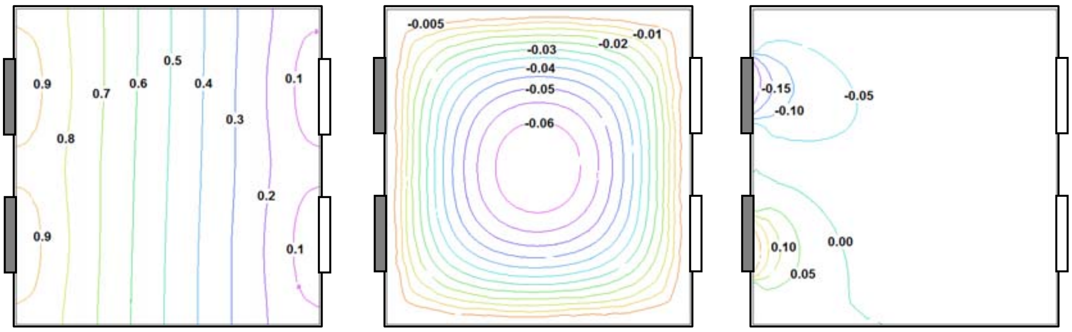

(a) Case 1

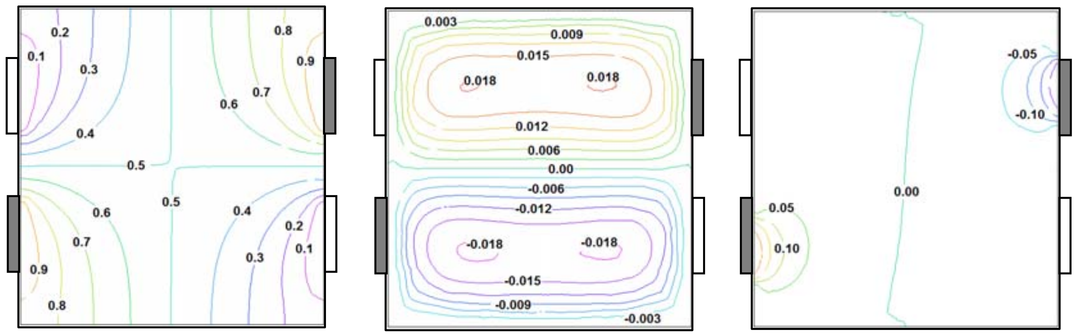

(b) Case 2

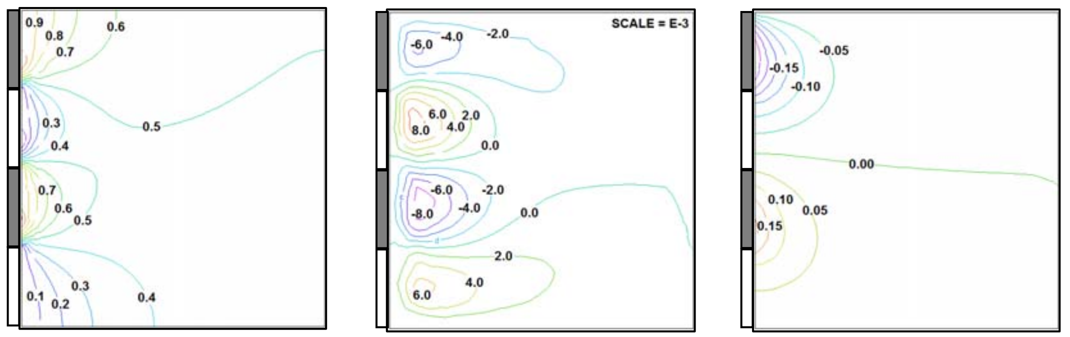

(c) Case 3

Figure 4. Isotherms (left), streamlines (center), and heatlines (right) for different arrangement of two source–sink pairs with $Ra = 10^6$, $Pr = 0.71$ and $Da = 10^{-6}$

source is transported to the bottom sink on the opposite side by the lower clockwise flow. It is also obvious that more heat is transported from the bottom source than the top source. For the sources and sinks alternately are located on the same sidewall in Case 3, their buoyancies are fully decomposed and therefore four eddies appear in the enclosure. Heatlines indicate that the heat from the top source is transported to only one sink along the flow direction. The heat from the bottom source is transported to two adjacent sinks in two directions, one towards the top sink by anti-clockwise flow and the other towards the bottom sink by clockwise flow.

Figure 3 shows the fluid flow and heat transfer characteristics and also heat transport structures by isotherms, streamlines, and heatlines for different arrangements of two source–sink pairs with $Ra = 10^6$, $Pr = 0.71$ and $Da = 10^{-4}$. The numerical results are similar to previous $Da = 10^{-1}$. Indeed, the fluid is driven from the sources to the sinks, which creates one eddy in Case 1, two eddies in Case 2 and four eddies in Case 3, and heatlines show that more heat is transferred from the bottom source than the top source. Since Da decreases, the intensity of fluid motion for $Da = 10^{-4}$ is weaker than $Da = 10^{-1}$.

Figure 4 shows the fluid flow and heat transfer characteristics and also heat transport structures by isotherms, streamlines, and heatlines for different arrangement of two source–sink pairs with $Ra = 10^6$, $Pr = 0.71$ and $Da = 10^{-6}$. The numerical results are similar to previous $Da = 10^{-4}$. Indeed, the fluid is driven from the sources to the sinks, which creates one eddy in Case 1, two eddies in Case 2 and four eddies in Case 3, and heatlines show that more heat is transferred from the bottom source than the top source. Since Da is very low, the distribution of heatlines is less than former result.

4 Conclusion

The objective of the present investigation is to study the problem of the fundamental fluid flow and heat transfer for natural convection in a two-dimensional square cavity with discrete two source–sink pairs on the vertical sidewalls. The arrangement of the sources and sinks changes from the separated modes to staggered modes. Discrete sources and sinks of the heat transfer in enclosures can be increased by splitting the sources and sinks into smaller segments and then place them alternately on the same sidewall in order to create the largest number of eddies in the enclosure. However the optimal design needs further investigation.

Acknowledgements

This research would not be possible without the support of Department of Mathematics, Faculty of Science, Khon Kaen University, and the Human Resource Development in Science Project (Science Achievement Scholarship of Thailand, SAST).

References

[1] P. H. Oosthuizen and D. Naylor, An introduction to convective heat transfer analysis, McGraw Hill, New York, 1999.

[2] T. Basak, S. Roy, T. Paul, and I. Pop, Natural convection in a square cavity filled with a porous medium: effects of various thermal boundary conditions, Int. J. Heat Mass Transfer, **49** (2006), 1430–1441.
[3] Q. H. Deng, Fluid flow and heat transfer characteristics of natural convection in square cavities due to discrete source–sink pairs, Int. J. Heat Mass Transfer, **51** (2008), 5949–5957.
[4] R. S. Kaluri, T. Basak, and S. Roy, Heatline approach for visualization of heat flow and efficient thermal mixing with discrete heat sources, Int. J. Heat Mass Transfer, **53** (2010), 3241–3261.
[5] J. N. Reddy, An Introduction to the Finite Element Method, 3rd Ed, McGraw-Hill Press, New York, 2006.
[6] G. K. Batchelor, An Introduction to Fluid Dynamics, Cambridge University Press, 1993.
[7] S. Kimura and A. Bejan, The heatline visualization of convective heat-transfer, ASME J. Heat Transfer, **105** (1983), 916–919.

Received: March, 2012